Proceedings of 10th International Conference on Precision, Meso, Micro and Nano Engineering (COPEN 10)
December 07 – 09, 2017, Indian Institute of Technology Madras, Chennai – 600 036 INDIA

Numerical Simulation and Comparative Study of Tool Profiles and Their Effect on Performance of Friction Stir Welding

Pratyush Kar*, Abhishek Ankolekar, P Vamsi Krishna
Department of Mechanical Engineering, National Institute of Technology, Warangal

Abstract

The present work focuses on comparing various tool profiles for heat generation and material flow capabilities in the partial stick-slip condition of FSW process. A model with different tool profiles is generated according to the required geometry. The continuity, momentum and energy equations are solved at every mesh cell, with suitable boundary conditions given to the various surfaces of the geometry. The values of the shear stress and heat fluxes at the various boundaries are entered based on the selected condition. The observations were made on, heat generation and material flow around the workpiece in the various interfacial conditions.

Keywords: friction stir welding, numerical modelling, fluent

1. INTRODUCTION

FSW is a complex process which requires detailed understanding of the process parameters. Computational tools are useful in such cases to derive the relation between input and output parameters. Responses like temperature profiles, material flow velocity and strain rates can be used for analysis of the process. Many researchers are working on the process of friction stir welding including both experimental and simulation. Ramanjaneyulu et al [1] formulated a mathematical model with process parameters and tool geometry to predict the responses of friction stir welds of AA2014-T6 aluminium alloy. The responses recorded were yield strength, tensile strength and ductility. Raza Moshwan et al. [2] investigated the effect of tool rotational speed on FSW of 3 mm thick AA5052-O aluminium alloy plates by using a constant traverse speed of 120 mm/min and varying the rotational speeds from 800 to 3000 rpm. It was observed that all speeds gave sound welds except at 3000 rpm. The maximum tensile strength of 132 MPa was obtained at 1000 rpm. Dongxiao Li et al [3] investigated the stationary shoulder friction stir welding for the AA6061-T6 alloy, with the shoulder stationary and the pin rotating, to generate heat. It was observed that the weld traverse section had a narrower thermo-mechanically affected zone (TMAZ) and heat affected zone (HAZ) as compared to conventional FSW. The microstructures were also more symmetrical and homogeneous.

In modelling and simulation of FSW process significant research has been done. Zhao Zhang et al. [4] created a numerical model for the FSW process taking a cylindrical and conical tool with different shoulder and tool diameters and investigated the effect of shoulder and pin diameters on material flow and heat generation. Hasan et al. [5] created a numerical model for the FSW process taking a worn and an unworn tool considering the variable speeds at shoulder region and variable nature of viscosity for AA7020 alloy. The model is simulated for strain rate at different locations and observed that in the worn tool, due to reduction in stirring action, material flow is hampered and the heat generation reduced. Schmidt et al. [6] created a new thermo-pseudo-mechanical model considering the partial sticking and sliding condition. The simulated model concluded that temperature-dependent yield stress of the weld material controlled the heat generation. Su et al. [7] developed a model for the calculation of friction coefficient, slip rate and heat generation for a conical and tri flat tool. His model suggested that heat generation is same for both the tools and stirring action is more in tri flat tool in comparison to the former one. Arora *et al.* [8] created a mathematical model to design a tool shoulder diameter based on the principle of maximum utilization of supplied torque for traction. Mehta *et al.*, [9] presented a methodology to analytically estimate the rate of heat generation for the tools with polygonal pins. A three-dimensional heat transfer analysis of FSW is carried out using FEA. The computed temperature field from the heat transfer model is used to estimate the torque, traverse force and the mechanical stresses experienced by regular triangular, square, pentagon and hexagon pins following the principles of solid mechanics. The computed results show that the peak temperature experienced by the tool pin increases with the number of pin sides.

*corresponding author, E-mail: pratyushkar@icloud.com

2. MODELLING AND SIMULATION

2.1 Material Properties

Material properties such as density, specific heat, thermal conductivity and viscosity are used in present study. Material viscosity is taken as the function of temperature and strain rate, other properties are taken as constant values. UDF formulations are used for calculating the material viscosity, Zener-Hollomon parameter and flow stress values. Material constants required during the calculations are taken from [10]

$$\sigma_f = \frac{1}{\alpha} sinh^{-1}\left[\left(\frac{z}{A}\right)^{\frac{1}{n}}\right] \quad (1)$$

$$z = \dot{\varepsilon} e^{\frac{Q}{RT}} \quad (2)$$

$$\mu = \frac{\sigma_f}{3\dot{\varepsilon}} \quad (3)$$

ISBN: 978-93-80689-28-9

Where A, α and n are material constants, Z is Zener - Hollomon parameter, Q is activation energy, R is Universal gas constant and t is the Temperature.

2.2 Boundary Conditions

Since the tool is rotating at some angular velocity, the material of the workpiece in contact with the tool may also rotate along with it at the same angular velocity or less than that. In order to account for this variation, the friction contact state variable (δ) is used [7].

$$\delta = 0.2 + 0.6\left(1 - e^{-\frac{\delta_o \omega r}{\omega_o R s}}\right) \quad (4)$$

The plain sliding condition occurs when δ=0, which means the velocity of the material at the interface is zero. The shear yield stress (τ_{yield}) exceeds the contact shear stress ($\tau_{contact}$) in this case and there is no flow of interface material.

$$\text{Shear Stress} = \tau = \mu P \quad (5)$$

Pure sticking occurs when δ=1, i.e., the interface matrix rotates at a velocity equal to the tool velocity and $\tau_{contact}$ exceeds τ_{yield} in this case, leading to high plastic deformation at the interface.

Partial sticking-sliding behaviour occurs when the value of δ is between 0 and 1. The material at the interface rotates at a velocity lesser than the tool rotational velocity. $\tau_{contact}$ equals τ_{yield} in this case, and due to the difference in relative velocity of the material and the tool at different angular positions leads to some portions being under stick condition and some portions under partial sliding condition.

$$\text{Shear Stress} = [(1-\delta)\eta\tau + \delta\mu P] \quad (6)$$

To carry out flow in the workpiece, the inlet and outlet should be present. The inlet velocity is taken as the weld velocity

$$u = u_{weld},\ v = 0,\ w = 0 \quad (7)$$

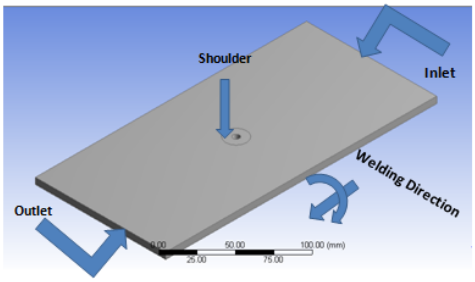

Fig-1 Boundary conditions on workpiece

where u, v and w represent the velocity magnitudes in the x-direction, y-direction and z-direction respectively; u_{weld} is the welding velocity. The velocity at the shoulder and pin region is considered as

$$u_i = (1-\delta)(r w \sin\theta - u_{weld}) \quad (8)$$

$$v_i = (1-\delta)(r w \cos\theta) \quad (9)$$

$$w_i = 0 \quad (10)$$

The heat generation in the sliding condition is

$$Q_1 = \frac{2}{3}\pi(1-\delta)\omega\mu P R_s \quad (11)$$

And the heat generation in the partial sticking condition is

$$Q_2 = [(1-\delta)\eta\tau + \delta\mu P](1-\delta)R_s\omega \quad (12)$$

Here, τ is the shear stress, μ coefficient of friction and P is the plunge pressure.

In order to know the velocity at each point in the fluid field and temperature distribution in the fluid, continuity, momentum and energy equations are solved. These equations are solved at every mesh cell.

3. VALIDATION OF THE MODEL:

Model is developed in ANSYS workbench and analysed using fluent. Material of the workpiece is defined with constant material properties like thermal conductivity and specific heat, in engineering data and allocated to workpiece. Different regions like shoulder region, pin side region etc generated in model. Meshing of the model is done by using tetrahedral elements. Laminar flow of material is considered for the present analysis. Contact between the tool and workpiece interface is assumed to be partial stick-slip condition. Momentum and heat boundary conditions are given to the particular regions as per requirement. Temperature profiles, material flow velocity are considered as performance parameters. The material is selected to be a fluid of Non-Newtonian type with a viscosity which varies with temperature and pressure. A UDF is defined for viscosity property input.

Generation of heat occurs due to rotation of tool against the workpiece, which leads to plasticizing the material. The plasticized material rotates along with the tool. Consequently, the maximum velocity is obtained based on the ratio of shoulder diameter to pin diameter, since heat generation also depends on this ratio. From the figure 2, the velocity increases as distance increases from the centre.

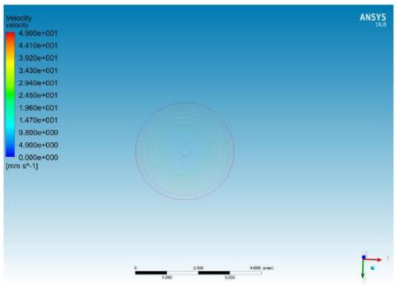

Fig-2 velocity distribution at tool bottom

The present model gives the maximum velocity value as 49 mm/min, while the maximum velocity from the Hasan et al [5] model is 43.6 mm/min. having a percentage error of 12.3%. The distribution of velocity in the present model and the Hasan model is similar, as shown in figure 3. Hasan considered a cylindrical tool pin with threads, and the meshing elements used

were prism and triangle. Due to these differences, the velocity in the current model is higher than the Hasan model.

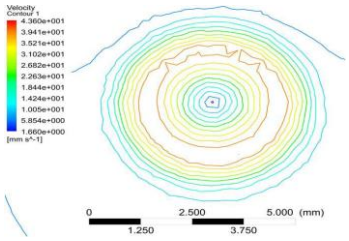

Fig-3 Hasan Model, velocity distribution at pin bottom

4. RESULTS AND DISCUSSION

In this work, various tool geometries are considered to study the material flow and heat generation. The shape of tools used are presented in fig 4.

Conical pin Square pin Triangular pin Cylindrical pin

Fig-4 different tool profiles 3D model

To study the effect of tool rotation speed, feed rate and plunge pressure on temperature distribution, multiple models are generated with different tool geometries and solved at different conditions. The variation of temperature with respect to rotation speed is derived by keeping feed rate and plunge pressure constant. One such condition of input parameters are given in the Table 1. The effect of different shapes are observed mainly on localized heating and material flow. Tool geometry is the most influential aspect of process development. In the initial stage of tool plunge, the heating results primarily from the friction between pin and work piece. The tool is plunged till the shoulder touches the workpiece. The friction between the shoulder and workpiece results in more amount of heat generation. The second function of the tool is to stir and move the material. The uniformity of microstructure and properties as well as process loads is governed by the tool design. The relationship between the static volume and dynamic volume decides the path for the flow of plasticized material from the leading edge to the trailing edge of the rotating tool.

Table -1 input parameters for modelling

S. No.	Boundary	Condition
1	Inlet velocity	44 mm/min
2	Shoulder Region	Viscosity UDF
3	Heat generation at shoulder	7.91 MW/m2
4	H.G. at pin lateral surface	1.17 MW/m2
5	H.G at pin bottom	1.04 MW/m2
6	Shear stress at shoulder region	28.92 MPa
7	Shear stress at pin bottom	24.87 MPa
8	Yield Stress	63.877 MPa
9	Plunge pressure	17 MPa

In the present work, the dimensions of the workpiece are 250*120*6 mm^3.The depth of penetration of the tool is 5.8 mm for all geometries. Simulations are run for each profile with input conditions as specified in table-1. The temperature distribution and material flow velocity are shown on different planes to visualize the effect of tool shape on TMAZ, HAZ.

4.1 TEMPERATURE DISTRIBUTION

To show the heat generation during process, different planes are selected and the variation of temperature along those planes are displayed though temperature contour plots along those planes.

4.1.1 Conical pin

For this conical pin, top diameter of the cone is 6 mm and bottom dimeter is 3 mm. The height of the pin is 5.8 mm. The shoulder dimeter is 19 mm.

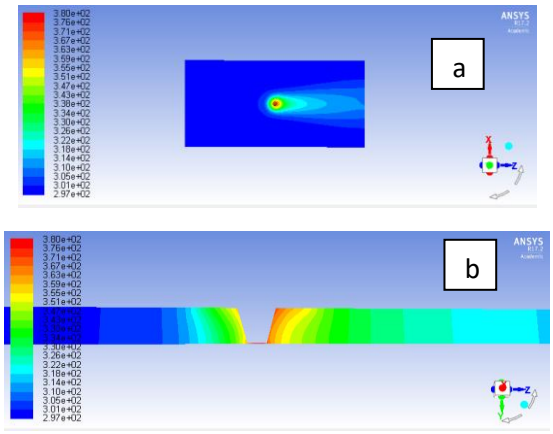

Fig-5 Temperature distribution for conical pin in longitudinal direction (a) on top surface and (b) on shoulder surface, pin bottom surface, pin side surface

The temperature contour plot shows (fig 5) a narrow HAZ which results in better mechanical properties of the joint. HAZ is also influenced by the weld velocity. The maximum temperature raise is 380 K.

4.1.2 Square pin

The cross section of the pin is 5*5 mm^2 and height of the pin is 5.8 mm. The shoulder diameter is same as conical pin. Same input conditions as that of conical pin are applied and resulting temperature contour is shown in fig 6.

From the two contour plots it is observed that the maximum temperature raise is 484 K which is higher than the conical pin. The HAZ is small and temperature distribution is uniform along the pin. As the cross-sectional area is more than the conical pin, by providing same heat flux it results in more temperature raise.

(a)

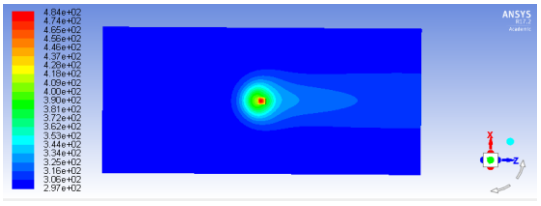

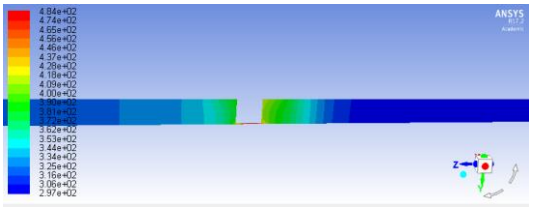

b)

Fig-6 Temperature distribution for square pin in longitudinal direction (a) on top surface and (b) on shoulder surface, pin bottom surface, pin side surface

4.1.3 Cylindrical pin

The dimeter of cylindrical pin is 5 mm and height is 5.8 mm. The input conditions are same as shown in table-1. The temperature contour obtained is shown in fig 7.

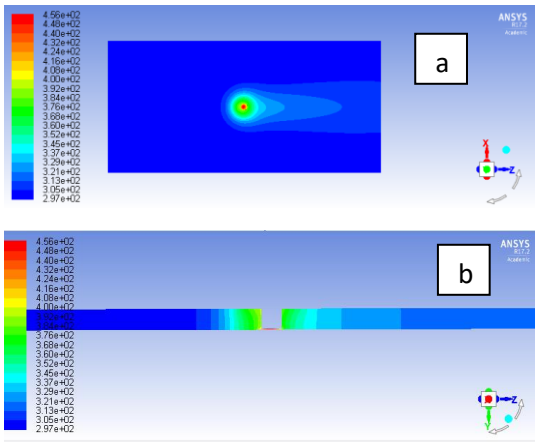

Fig-7 Temperature distribution for cylindrical pin in longitudinal direction (a) on top surface and (b)on shoulder surface, pin bottom surface, pin side surface

From the temperature contour, the maximum temperature raise is 456 K which is lesser than square pin but higher than conical pin. The temperature is more localized. The surface area is less as compared to the square pin, so it results less heat generation.

4.1.4Triangular pin

For triangular pin, an equilateral triangle having side length 5 mm is taken and the height is same as all previous cases as 5.8 mm. The temperature so obtained is shown in fig 8. With same input conditions, much increase in temperature is observed which is about 557 K. This high temperature is limited to pin bottom area, visible in the contour. The temperature distribution is also wider than all other tool profiles.

4.2 MATERIAL FLOW BEHAVIOUR

The flow of material depends upon the type of contact occurring between tool and workpiece interface during the process. Partial stick-slip condition consideration combines the effect of stick and slip condition. If stick condition has occurred during the process then with increase in rotational speed, material flow velocity will also increase because of sufficient heat generation due to plastic deformation. Material flow velocity profiles in FSW gives the quality of process in terms of distribution of material. The material flow velocity is obtained by taking the same input conditions as stated in table-1. The resulting flow pattern for different tool profiles is shown in the figures 9-12.

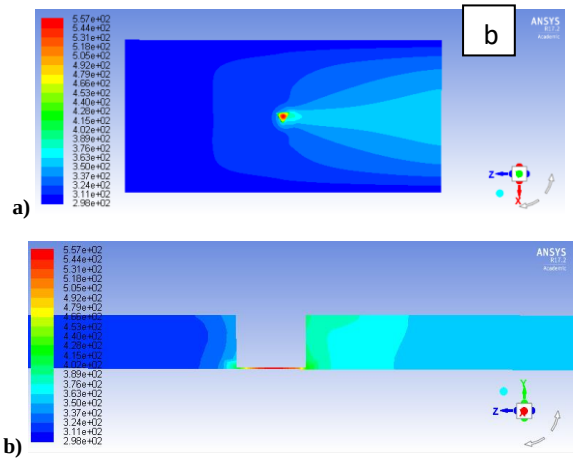

a)

b)

Fig-8 Temperature distribution for conical pin in longitudinal direction (a) on top surface and (b) on shoulder surface, pin bottom surface, pin side surface

The selected planes for this velocity vector distribution are top surface, shoulder region, pin bottom surface and in longitudinal direction. The maximum flow velocity of the material obtained for conical, square, cylindrical and triangular pins respectively are 0.04m/sec,0.05m/sec,0.051m/sec and 0.136m/sec. The flow around the triangular pin profile is much complex than the other profiles. For the triangular profile, the flow pattern is constantly changing and maximum velocity is obtained at the edge of the flat area. The stirring action is more complex than the other profiles.

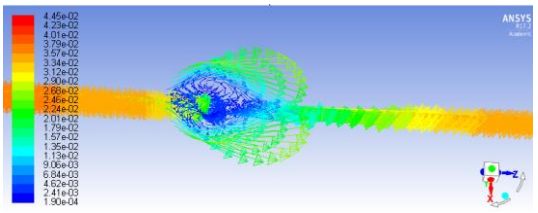

Fig 9: Material flow velocity around shoulder and pin region of a conical tool

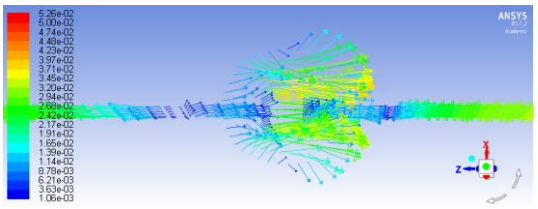

Fig 10: Material flow velocity around shoulder and pin region of a square tool

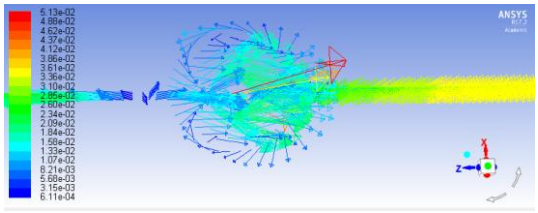

Fig 11: Material flow velocity around shoulder and pin region of a cylindrical tool

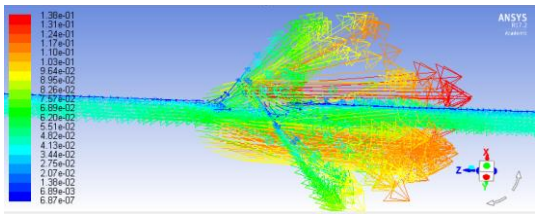

Fig 12: Material flow velocity around shoulder and pin region of a triangular tool

5. CONCLUSION

Current work emphasizes on the tool profile effect of FSW while joining Al6063 alloy. The thermal and velocity boundary conditions at the pin bottom, pin side surface and shoulder area are given more importance. Partial sticking/sliding contact condition is considered, which is more approximate with the real FSW process. The temperature distribution, the material flow and deformation region, especially the flow characteristics, on various pin profiles during the process is analysed.

It is found that the ‘‘stir action’’ of triangular is more drastic than that of square, conical and cylindrical tool profiles. The pin side flat area changes the distribution feature of strain rate and viscosity, and enlarges the deformation region.

The flow pattern and temperature rise are highly influenced by the presence of flats in the tool as this additional feature provides more pulsing action. Hence, temperature rise is more for square tool when compared between conical, cylindrical and square shaped tool.

References

[1] Ramanjaneyulu Kadaganchi, Optimization of process parameters of aluminum alloy AA 2014-T6 friction stir welds by response surface methodology, Defence Technology 11 (2015) 209-219.

[2] Raza Moshwan*et al.*, Effect of tool rotational speed on force generation, microstructure and mechanical properties of friction stir welded Al–Mg–Cr–Mn (AA5052-O) alloy, Materials and Design 66 (2015) 118–128.

[3] Dongxiao Li *et al.* Effect of welding parameters on microstructure and mechanicalproperties of AA6061-T6 butt welded joints by stationary shoulder friction stir welding

[4] Zhao ZHANG, Qi WU, Hong-wu ZHANG, Numerical studies of effect of tool sizes and pin shapes on friction stir welding of AA2024-T3 alloy, Trans. Nonferrous Met. Soc. China 24(2014) 3293-3301.

[5] A.F. Hasan *et al.*, A numerical comparison of the flow behaviour in Friction Stir Welding (FSW) using unworn and worn tool geometries, Materials and Design 87 (2015) 1037–1046.

[6] H. Schmidt, J. Hattel, J. Wert, An analytical model for the heat generation in friction stir welding, Model. Simul. Mater. Sci. Eng. 12 (1) (2004) 143.

[7] H. Su, *et al.*, Numerical modeling for the effect of pin profiles on thermal and material flow characteristics in friction stir welding, Mater. Des. 77 (2015) 114–125.

[8] A. Arora, et al., Torque, power requirement and stir zone geometry in friction stir welding through modeling and experiments, Scr. Mater. 60 (1) (2009) 13 16.

[9] M. Mehta *et al.*, Numerical modeling of friction stir welding using the tools with polygonal pins, Defence Technology 11 (2015) 229-236.53

[10] Chun-lei GAN, Kai-hong ZHENG, Wen-jun QI, Meng-jun WANG Constitutive equations for high temperature flow stress prediction of 6063 Al alloy considering compensation of strain. Trans. Nonferrous Met. Soc. China 24(2014) 3486−3491.

[11] Judy et. al., Material flow modification in a FSW through introduction of flats Metallurgical and Materials Transactions B, 2016, 47B: 720-730